EUROPEAN ORGANIZATION FOR NUCLEAR RESEARCH (CERN)

CERN-PH-EP-2014-115
LHCb-PAPER-2014-020
3 June 2014

Observation of the $\Lambda_b^0 \to J/\psi\, p\pi^-$ decay

The LHCb collaboration[†]

Abstract

The first observation of the Cabibbo-suppressed decay $\Lambda_b^0 \to J/\psi p\pi^-$ is reported using a data sample of proton-proton collisions at 7 and 8 TeV, corresponding to an integrated luminosity of 3 fb^{-1}. A prominent signal is observed and the branching fraction relative to the decay mode $\Lambda_b^0 \to J/\psi pK^-$ is determined to be

$$\frac{\mathcal{B}(\Lambda_b^0 \to J/\psi p\pi^-)}{\mathcal{B}(\Lambda_b^0 \to J/\psi pK^-)} = 0.0824 \pm 0.0025\,(\text{stat}) \pm 0.0042\,(\text{syst}).$$

A search for direct CP violation is performed. The difference in the CP asymmetries between these two decays is found to be

$$\mathcal{A}_{CP}(\Lambda_b^0 \to J/\psi p\pi^-) - \mathcal{A}_{CP}(\Lambda_b^0 \to J/\psi pK^-) = (+5.7 \pm 2.4\,(\text{stat}) \pm 1.2\,(\text{syst}))\%,$$

which is compatible with CP symmetry at the 2.2σ level.

Published in JHEP 07 (2014) 103

[†]Authors are listed on the following pages.

LHCb collaboration

R. Aaij[41], B. Adeva[37], M. Adinolfi[46], A. Affolder[52], Z. Ajaltouni[5], S. Akar[6], J. Albrecht[9], F. Alessio[38], M. Alexander[51], S. Ali[41], G. Alkhazov[30], P. Alvarez Cartelle[37], A.A. Alves Jr[25,38], S. Amato[2], S. Amerio[22], Y. Amhis[7], L. An[3], L. Anderlini[17,g], J. Anderson[40], R. Andreassen[57], M. Andreotti[16,f], J.E. Andrews[58], R.B. Appleby[54], O. Aquines Gutierrez[10], F. Archilli[38], A. Artamonov[35], M. Artuso[59], E. Aslanides[6], G. Auriemma[25,n], M. Baalouch[5], A. Bǎbeanu[38,q], S. Bachmann[11], J.J. Back[48], A. Badalov[36], V. Balagura[31], W. Baldini[16], R.J. Barlow[54], C. Barschel[38], S. Barsuk[7], W. Barter[47], V. Batozskaya[28], V. Battista[39], A. Bay[39], L. Beaucourt[4], J. Beddow[51], F. Bedeschi[23], I. Bediaga[1], S. Belogurov[31], K. Belous[35], I. Belyaev[31], E. Ben-Haim[8], G. Bencivenni[18], S. Benson[38], J. Benton[46], A. Berezhnoy[32], R. Bernet[40], M.-O. Bettler[47], M. van Beuzekom[41], A. Bien[11], S. Bifani[45], T. Bird[54], A. Bizzeti[17,i], P.M. Bjørnstad[54], T. Blake[48], F. Blanc[39], J. Blouw[10], S. Blusk[59], V. Bocci[25], A. Bondar[34], N. Bondar[30,38], W. Bonivento[15,38], S. Borghi[54], A. Borgia[59], M. Borsato[7], T.J.V. Bowcock[52], E. Bowen[40], C. Bozzi[16], T. Brambach[9], J. van den Brand[42], J. Bressieux[39], D. Brett[54], M. Britsch[10], T. Britton[59], J. Brodzicka[54], N.H. Brook[46], H. Brown[52], A. Bursche[40], G. Busetto[22,s], J. Buytaert[38], S. Cadeddu[15], R. Calabrese[16,f], M. Calvi[20,k], M. Calvo Gomez[36,p], A. Camboni[36], P. Campana[18,38], D. Campora Perez[38], A. Carbone[14,d], G. Carboni[24,l], R. Cardinale[19,38,j], A. Cardini[15], H. Carranza-Mejia[50], L. Carson[50], K. Carvalho Akiba[2], G. Casse[52], L. Cassina[20], L. Castillo Garcia[38], M. Cattaneo[38], Ch. Cauet[9], R. Cenci[58], M. Charles[8], Ph. Charpentier[38], S. Chen[54], S.-F. Cheung[55], N. Chiapolini[40], M. Chrzaszcz[40,26], K. Ciba[38], X. Cid Vidal[38], G. Ciezarek[53], P.E.L. Clarke[50], M. Clemencic[38], H.V. Cliff[47], J. Closier[38], V. Coco[38], J. Cogan[6], E. Cogneras[5], P. Collins[38], A. Comerma-Montells[11], A. Contu[15], A. Cook[46], M. Coombes[46], S. Coquereau[8], G. Corti[38], M. Corvo[16,f], I. Counts[56], B. Couturier[38], G.A. Cowan[50], D.C. Craik[48], M. Cruz Torres[60], S. Cunliffe[53], R. Currie[50], C. D'Ambrosio[38], J. Dalseno[46], P. David[8], P.N.Y. David[41], A. Davis[57], K. De Bruyn[41], S. De Capua[54], M. De Cian[11], J.M. De Miranda[1], L. De Paula[2], W. De Silva[57], P. De Simone[18], D. Decamp[4], M. Deckenhoff[9], L. Del Buono[8], N. Déléage[4], D. Derkach[55], O. Deschamps[5], F. Dettori[38], A. Di Canto[38], H. Dijkstra[38], S. Donleavy[52], F. Dordei[11], M. Dorigo[39], A. Dosil Suárez[37], D. Dossett[48], A. Dovbnya[43], K. Dreimanis[52], G. Dujany[54], F. Dupertuis[39], P. Durante[38], R. Dzhelyadin[35], A. Dziurda[26], A. Dzyuba[30], S. Easo[49,38], U. Egede[53], V. Egorychev[31], S. Eidelman[34], S. Eisenhardt[50], U. Eitschberger[9], R. Ekelhof[9], L. Eklund[51,38], I. El Rifai[5], Ch. Elsasser[40], S. Ely[59], S. Esen[11], H.-M. Evans[47], T. Evans[55], A. Falabella[16,f], C. Färber[11], C. Farinelli[41], N. Farley[45], S. Farry[52], RF Fay[52], D. Ferguson[50], V. Fernandez Albor[37], F. Ferreira Rodrigues[1], M. Ferro-Luzzi[38], S. Filippov[33], M. Fiore[16,f], M. Fiorini[16,f], M. Firlej[27], C. Fitzpatrick[38], T. Fiutowski[27], M. Fontana[10], F. Fontanelli[19,j], R. Forty[38], O. Francisco[2], M. Frank[38], C. Frei[38], M. Frosini[17,38,g], J. Fu[21,38], E. Furfaro[24,l], A. Gallas Torreira[37], D. Galli[14,d], S. Gallorini[22], S. Gambetta[19,j], M. Gandelman[2], P. Gandini[59], Y. Gao[3], J. Garofoli[59], J. Garra Tico[47], L. Garrido[36], C. Gaspar[38], R. Gauld[55], L. Gavardi[9], G. Gavrilov[30], E. Gersabeck[11], M. Gersabeck[54], T. Gershon[48], Ph. Ghez[4], A. Gianelle[22], S. Giani'[39], V. Gibson[47], L. Giubega[29], V.V. Gligorov[38], C. Göbel[60], D. Golubkov[31], A. Golutvin[53,31,38], A. Gomes[1,a], H. Gordon[38], C. Gotti[20], M. Grabalosa Gándara[5], R. Graciani Diaz[36], L.A. Granado Cardoso[38], E. Graugés[36], G. Graziani[17], A. Grecu[29], E. Greening[55], S. Gregson[47], P. Griffith[45], L. Grillo[11], O. Grünberg[62], B. Gui[59], E. Gushchin[33], Yu. Guz[35,38], T. Gys[38], C. Hadjivasiliou[59], G. Haefeli[39], C. Haen[38], S.C. Haines[47], S. Hall[53], B. Hamilton[58], T. Hampson[46], X. Han[11], S. Hansmann-Menzemer[11], N. Harnew[55],

S.T. Harnew[46], J. Harrison[54], T. Hartmann[62], J. He[38], T. Head[38], V. Heijne[41], K. Hennessy[52], P. Henrard[5], L. Henry[8], J.A. Hernando Morata[37], E. van Herwijnen[38], M. Heß[62], A. Hicheur[1], D. Hill[55], M. Hoballah[5], C. Hombach[54], W. Hulsbergen[41], P. Hunt[55], N. Hussain[55], D. Hutchcroft[52], D. Hynds[51], M. Idzik[27], P. Ilten[56], R. Jacobsson[38], A. Jaeger[11], J. Jalocha[55], E. Jans[41], P. Jaton[39], A. Jawahery[58], F. Jing[3], M. John[55], D. Johnson[55], C.R. Jones[47], C. Joram[38], B. Jost[38], N. Jurik[59], M. Kaballo[9], S. Kandybei[43], W. Kanso[6], M. Karacson[38], T.M. Karbach[38], S. Karodia[51], M. Kelsey[59], I.R. Kenyon[45], T. Ketel[42], B. Khanji[20], C. Khurewathanakul[39], S. Klaver[54], O. Kochebina[7], M. Kolpin[11], I. Komarov[39], R.F. Koopman[42], P. Koppenburg[41,38], M. Korolev[32], A. Kozlinskiy[41], L. Kravchuk[33], K. Kreplin[11], M. Kreps[48], G. Krocker[11], P. Krokovny[34], F. Kruse[9], W. Kucewicz[26,o], M. Kucharczyk[20,26,38,k], V. Kudryavtsev[34], K. Kurek[28], T. Kvaratskheliya[31], V.N. La Thi[39], D. Lacarrere[38], G. Lafferty[54], A. Lai[15], D. Lambert[50], R.W. Lambert[42], E. Lanciotti[38], G. Lanfranchi[18], C. Langenbruch[38], B. Langhans[38], T. Latham[48], C. Lazzeroni[45], R. Le Gac[6], J. van Leerdam[41], J.-P. Lees[4], R. Lefèvre[5], A. Leflat[32], J. Lefrançois[7], S. Leo[23], O. Leroy[6], T. Lesiak[26], B. Leverington[11], Y. Li[3], M. Liles[52], R. Lindner[38], C. Linn[38], F. Lionetto[40], B. Liu[15], G. Liu[38], S. Lohn[38], I. Longstaff[51], J.H. Lopes[2], N. Lopez-March[39], P. Lowdon[40], H. Lu[3], D. Lucchesi[22,s], H. Luo[50], A. Lupato[22], E. Luppi[16,f], O. Lupton[55], F. Machefert[7], I.V. Machikhiliyan[31], F. Maciuc[29], O. Maev[30], S. Malde[55], G. Manca[15,e], G. Mancinelli[6], J. Maratas[5], J.F. Marchand[4], U. Marconi[14], C. Marin Benito[36], P. Marino[23,u], R. Märki[39], J. Marks[11], G. Martellotti[25], A. Martens[8], A. Martín Sánchez[7], M. Martinelli[41], D. Martinez Santos[42], F. Martinez Vidal[64], D. Martins Tostes[2], A. Massafferri[1], R. Matev[38], Z. Mathe[38], C. Matteuzzi[20], A. Mazurov[16,f], M. McCann[53], J. McCarthy[45], A. McNab[54], R. McNulty[12], B. McSkelly[52], B. Meadows[57], F. Meier[9], M. Meissner[11], M. Merk[41], D.A. Milanes[8], M.-N. Minard[4], N. Moggi[14], J. Molina Rodriguez[60], S. Monteil[5], M. Morandin[22], P. Morawski[27], A. Mordà[6], M.J. Morello[23,u], J. Moron[27], A.-B. Morris[50], R. Mountain[59], F. Muheim[50], K. Müller[40], R. Muresan[29], M. Mussini[14], B. Muster[39], P. Naik[46], T. Nakada[39], R. Nandakumar[49], I. Nasteva[2], M. Needham[50], N. Neri[21], S. Neubert[38], N. Neufeld[38], M. Neuner[11], A.D. Nguyen[39], T.D. Nguyen[39], C. Nguyen-Mau[39,r], M. Nicol[7], V. Niess[5], R. Niet[9], N. Nikitin[32], T. Nikodem[11], A. Novoselov[35], D.P. O'Hanlon[48], A. Oblakowska-Mucha[27], V. Obraztsov[35], S. Oggero[41], S. Ogilvy[51], O. Okhrimenko[44], R. Oldeman[15,e], G. Onderwater[65], M. Orlandea[29], J.M. Otalora Goicochea[2], P. Owen[53], A. Oyanguren[64], B.K. Pal[59], A. Palano[13,c], F. Palombo[21,v], M. Palutan[18], J. Panman[38], A. Papanestis[49,38], M. Pappagallo[51], C. Parkes[54], C.J. Parkinson[9,45], G. Passaleva[17], G.D. Patel[52], M. Patel[53], C. Patrignani[19,j], A. Pazos Alvarez[37], A. Pearce[54], A. Pellegrino[41], M. Pepe Altarelli[38], S. Perazzini[14,d], E. Perez Trigo[37], P. Perret[5], M. Perrin-Terrin[6], L. Pescatore[45], E. Pesen[66], K. Petridis[53], A. Petrolini[19,j], E. Picatoste Olloqui[36], B. Pietrzyk[4], T. Pilař[48], D. Pinci[25], A. Pistone[19], S. Playfer[50], M. Plo Casasus[37], F. Polci[8], A. Poluektov[48,34], E. Polycarpo[2], A. Popov[35], D. Popov[10], B. Popovici[29], C. Potterat[2], E. Price[46], J. Prisciandaro[39], A. Pritchard[52], C. Prouve[46], V. Pugatch[44], A. Puig Navarro[39], G. Punzi[23,t], W. Qian[4], B. Rachwal[26], J.H. Rademacker[46], B. Rakotomiaramanana[39], M. Rama[18], M.S. Rangel[2], I. Raniuk[43], N. Rauschmayr[38], G. Raven[42], S. Reichert[54], M.M. Reid[48], A.C. dos Reis[1], S. Ricciardi[49], S. Richards[46], M. Rihl[38], K. Rinnert[52], V. Rives Molina[36], D.A. Roa Romero[5], P. Robbe[7], A.B. Rodrigues[1], E. Rodrigues[54], P. Rodriguez Perez[54], S. Roiser[38], V. Romanovsky[35], A. Romero Vidal[37], M. Rotondo[22], J. Rouvinet[39], T. Ruf[38], F. Ruffini[23], H. Ruiz[36], P. Ruiz Valls[64], G. Sabatino[25,l], J.J. Saborido Silva[37], N. Sagidova[30], P. Sail[51], B. Saitta[15,e], V. Salustino Guimaraes[2], C. Sanchez Mayordomo[64],

B. Sanmartin Sedes[37], R. Santacesaria[25], C. Santamarina Rios[37], E. Santovetti[24,l], M. Sapunov[6], A. Sarti[18,m], C. Satriano[25,n], A. Satta[24], D.M. Saunders[46], M. Savrie[16,f], D. Savrina[31,32], M. Schiller[42], H. Schindler[38], M. Schlupp[9], M. Schmelling[10], B. Schmidt[38], O. Schneider[39], A. Schopper[38], M.-H. Schune[7], R. Schwemmer[38], B. Sciascia[18], A. Sciubba[25], M. Seco[37], A. Semennikov[31], I. Sepp[53], N. Serra[40], J. Serrano[6], L. Sestini[22], P. Seyfert[11], M. Shapkin[35], I. Shapoval[16,43,f], Y. Shcheglov[30], T. Shears[52], L. Shekhtman[34], V. Shevchenko[63], A. Shires[9], R. Silva Coutinho[48], G. Simi[22], M. Sirendi[47], N. Skidmore[46], T. Skwarnicki[59], N.A. Smith[52], E. Smith[55,49], E. Smith[53], J. Smith[47], M. Smith[54], H. Snoek[41], M.D. Sokoloff[57], F.J.P. Soler[51], F. Soomro[39], D. Souza[46], B. Souza De Paula[2], B. Spaan[9], A. Sparkes[50], P. Spradlin[51], F. Stagni[38], M. Stahl[11], S. Stahl[11], O. Steinkamp[40], O. Stenyakin[35], S. Stevenson[55], S. Stoica[29], S. Stone[59], B. Storaci[40], S. Stracka[23,38], M. Straticiuc[29], U. Straumann[40], R. Stroili[22], V.K. Subbiah[38], L. Sun[57], W. Sutcliffe[53], K. Swientek[27], S. Swientek[9], V. Syropoulos[42], M. Szczekowski[28], P. Szczypka[39,38], D. Szilard[2], T. Szumlak[27], S. T'Jampens[4], M. Teklishyn[7], G. Tellarini[16,f], F. Teubert[38], C. Thomas[55], E. Thomas[38], J. van Tilburg[41], V. Tisserand[4], M. Tobin[39], S. Tolk[42], L. Tomassetti[16,f], D. Tonelli[38], S. Topp-Joergensen[55], N. Torr[55], E. Tournefier[4], S. Tourneur[39], M.T. Tran[39], M. Tresch[40], A. Tsaregorodtsev[6], P. Tsopelas[41], N. Tuning[41], M. Ubeda Garcia[38], A. Ukleja[28], A. Ustyuzhanin[63], U. Uwer[11], V. Vagnoni[14], G. Valenti[14], A. Vallier[7], R. Vazquez Gomez[18], P. Vazquez Regueiro[37], C. Vázquez Sierra[37], S. Vecchi[16], J.J. Velthuis[46], M. Veltri[17,h], G. Veneziano[39], M. Vesterinen[11], B. Viaud[7], D. Vieira[2], M. Vieites Diaz[37], X. Vilasis-Cardona[36,p], A. Vollhardt[40], D. Volyanskyy[10], D. Voong[46], A. Vorobyev[30], V. Vorobyev[34], C. Voß[62], H. Voss[10], J.A. de Vries[41], R. Waldi[62], C. Wallace[48], R. Wallace[12], J. Walsh[23], S. Wandernoth[11], J. Wang[59], D.R. Ward[47], N.K. Watson[45], D. Websdale[53], M. Whitehead[48], J. Wicht[38], D. Wiedner[11], G. Wilkinson[55], M.P. Williams[45], M. Williams[56], F.F. Wilson[49], J. Wimberley[58], J. Wishahi[9], W. Wislicki[28], M. Witek[26], G. Wormser[7], S.A. Wotton[47], S. Wright[47], S. Wu[3], K. Wyllie[38], Y. Xie[61], Z. Xing[59], Z. Xu[39], Z. Yang[3], X. Yuan[3], O. Yushchenko[35], M. Zangoli[14], M. Zavertyaev[10,b], L. Zhang[59], W.C. Zhang[12], Y. Zhang[3], A. Zhelezov[11], A. Zhokhov[31], L. Zhong[3], A. Zvyagin[38].

[1] *Centro Brasileiro de Pesquisas Físicas (CBPF), Rio de Janeiro, Brazil*
[2] *Universidade Federal do Rio de Janeiro (UFRJ), Rio de Janeiro, Brazil*
[3] *Center for High Energy Physics, Tsinghua University, Beijing, China*
[4] *LAPP, Université de Savoie, CNRS/IN2P3, Annecy-Le-Vieux, France*
[5] *Clermont Université, Université Blaise Pascal, CNRS/IN2P3, LPC, Clermont-Ferrand, France*
[6] *CPPM, Aix-Marseille Université, CNRS/IN2P3, Marseille, France*
[7] *LAL, Université Paris-Sud, CNRS/IN2P3, Orsay, France*
[8] *LPNHE, Université Pierre et Marie Curie, Université Paris Diderot, CNRS/IN2P3, Paris, France*
[9] *Fakultät Physik, Technische Universität Dortmund, Dortmund, Germany*
[10] *Max-Planck-Institut für Kernphysik (MPIK), Heidelberg, Germany*
[11] *Physikalisches Institut, Ruprecht-Karls-Universität Heidelberg, Heidelberg, Germany*
[12] *School of Physics, University College Dublin, Dublin, Ireland*
[13] *Sezione INFN di Bari, Bari, Italy*
[14] *Sezione INFN di Bologna, Bologna, Italy*
[15] *Sezione INFN di Cagliari, Cagliari, Italy*
[16] *Sezione INFN di Ferrara, Ferrara, Italy*
[17] *Sezione INFN di Firenze, Firenze, Italy*
[18] *Laboratori Nazionali dell'INFN di Frascati, Frascati, Italy*
[19] *Sezione INFN di Genova, Genova, Italy*
[20] *Sezione INFN di Milano Bicocca, Milano, Italy*
[21] *Sezione INFN di Milano, Milano, Italy*

[22] *Sezione INFN di Padova, Padova, Italy*
[23] *Sezione INFN di Pisa, Pisa, Italy*
[24] *Sezione INFN di Roma Tor Vergata, Roma, Italy*
[25] *Sezione INFN di Roma La Sapienza, Roma, Italy*
[26] *Henryk Niewodniczanski Institute of Nuclear Physics Polish Academy of Sciences, Kraków, Poland*
[27] *AGH - University of Science and Technology, Faculty of Physics and Applied Computer Science, Kraków, Poland*
[28] *National Center for Nuclear Research (NCBJ), Warsaw, Poland*
[29] *Horia Hulubei National Institute of Physics and Nuclear Engineering, Bucharest-Magurele, Romania*
[30] *Petersburg Nuclear Physics Institute (PNPI), Gatchina, Russia*
[31] *Institute of Theoretical and Experimental Physics (ITEP), Moscow, Russia*
[32] *Institute of Nuclear Physics, Moscow State University (SINP MSU), Moscow, Russia*
[33] *Institute for Nuclear Research of the Russian Academy of Sciences (INR RAN), Moscow, Russia*
[34] *Budker Institute of Nuclear Physics (SB RAS) and Novosibirsk State University, Novosibirsk, Russia*
[35] *Institute for High Energy Physics (IHEP), Protvino, Russia*
[36] *Universitat de Barcelona, Barcelona, Spain*
[37] *Universidad de Santiago de Compostela, Santiago de Compostela, Spain*
[38] *European Organization for Nuclear Research (CERN), Geneva, Switzerland*
[39] *Ecole Polytechnique Fédérale de Lausanne (EPFL), Lausanne, Switzerland*
[40] *Physik-Institut, Universität Zürich, Zürich, Switzerland*
[41] *Nikhef National Institute for Subatomic Physics, Amsterdam, The Netherlands*
[42] *Nikhef National Institute for Subatomic Physics and VU University Amsterdam, Amsterdam, The Netherlands*
[43] *NSC Kharkiv Institute of Physics and Technology (NSC KIPT), Kharkiv, Ukraine*
[44] *Institute for Nuclear Research of the National Academy of Sciences (KINR), Kyiv, Ukraine*
[45] *University of Birmingham, Birmingham, United Kingdom*
[46] *H.H. Wills Physics Laboratory, University of Bristol, Bristol, United Kingdom*
[47] *Cavendish Laboratory, University of Cambridge, Cambridge, United Kingdom*
[48] *Department of Physics, University of Warwick, Coventry, United Kingdom*
[49] *STFC Rutherford Appleton Laboratory, Didcot, United Kingdom*
[50] *School of Physics and Astronomy, University of Edinburgh, Edinburgh, United Kingdom*
[51] *School of Physics and Astronomy, University of Glasgow, Glasgow, United Kingdom*
[52] *Oliver Lodge Laboratory, University of Liverpool, Liverpool, United Kingdom*
[53] *Imperial College London, London, United Kingdom*
[54] *School of Physics and Astronomy, University of Manchester, Manchester, United Kingdom*
[55] *Department of Physics, University of Oxford, Oxford, United Kingdom*
[56] *Massachusetts Institute of Technology, Cambridge, MA, United States*
[57] *University of Cincinnati, Cincinnati, OH, United States*
[58] *University of Maryland, College Park, MD, United States*
[59] *Syracuse University, Syracuse, NY, United States*
[60] *Pontifícia Universidade Católica do Rio de Janeiro (PUC-Rio), Rio de Janeiro, Brazil, associated to* [2]
[61] *Institute of Particle Physics, Central China Normal University, Wuhan, Hubei, China, associated to* [3]
[62] *Institut für Physik, Universität Rostock, Rostock, Germany, associated to* [11]
[63] *National Research Centre Kurchatov Institute, Moscow, Russia, associated to* [31]
[64] *Instituto de Fisica Corpuscular (IFIC), Universitat de Valencia-CSIC, Valencia, Spain, associated to* [36]
[65] *KVI - University of Groningen, Groningen, The Netherlands, associated to* [41]
[66] *Celal Bayar University, Manisa, Turkey, associated to* [38]

[a] *Universidade Federal do Triângulo Mineiro (UFTM), Uberaba-MG, Brazil*
[b] *P.N. Lebedev Physical Institute, Russian Academy of Science (LPI RAS), Moscow, Russia*
[c] *Università di Bari, Bari, Italy*
[d] *Università di Bologna, Bologna, Italy*

[e] *Università di Cagliari, Cagliari, Italy*
[f] *Università di Ferrara, Ferrara, Italy*
[g] *Università di Firenze, Firenze, Italy*
[h] *Università di Urbino, Urbino, Italy*
[i] *Università di Modena e Reggio Emilia, Modena, Italy*
[j] *Università di Genova, Genova, Italy*
[k] *Università di Milano Bicocca, Milano, Italy*
[l] *Università di Roma Tor Vergata, Roma, Italy*
[m] *Università di Roma La Sapienza, Roma, Italy*
[n] *Università della Basilicata, Potenza, Italy*
[o] *AGH - University of Science and Technology, Faculty of Computer Science, Electronics and Telecommunications, Kraków, Poland*
[p] *LIFAELS, La Salle, Universitat Ramon Llull, Barcelona, Spain*
[q] *University of Utrecht, Utrecht, The Netherlands*
[r] *Hanoi University of Science, Hanoi, Viet Nam*
[s] *Università di Padova, Padova, Italy*
[t] *Università di Pisa, Pisa, Italy*
[u] *Scuola Normale Superiore, Pisa, Italy*
[v] *Università degli Studi di Milano, Milano, Italy*

1 Introduction

The study of b-baryon decays is of considerable interest both to probe the dynamics of heavy flavour decay processes and to search for the effects of physics beyond the Standard Model. Owing to their non-zero spin, b baryons provide the potential to improve the limited understanding of the helicity structure of the underlying Hamiltonian [1].

Beauty baryons are copiously produced at the LHC, where the Λ_b^0 baryon cross-section is about half of the size of the B^0 meson production in the forward region [2]. The ATLAS, CMS and LHCb collaborations measured the Λ_b^0 lifetime [3–5], and the masses of the ground [5, 6] and first excited states [7]. The Λ_b^0 polarisation has been measured and found to be compatible with zero [8]. The LHCb collaboration has studied Λ_b^0 decays to charmonium [8, 9], open charm [10, 11], charmless states [12] and final states induced by electroweak penguins [13]. No evidence for CP violation has been reported in decays of baryons. Searches with b-baryon decays have been performed with the decay channels $\Lambda_b^0 \to p\pi^-$, pK^- [14] and $K_S^0 p\pi^-$ [12]. The corresponding theoretical literature is still limited compared to that on B meson decays.

The study of $b \to c\bar{c}q$ decays can be used to constrain penguin pollution in the determination of the CP-violating phases in B^0 and B_s^0 mixing [15]. While decays originating from the $b \to c\bar{c}s$ transitions, such as $\Lambda_b^0 \to J/\psi\,\Lambda$ or $\Lambda_b^0 \to J/\psi\,pK^-$, are largely dominated by the tree amplitudes, penguins amplitudes are enhanced in Cabibbo-suppressed $b \to c\bar{c}d$ transitions, such as the $\Lambda_b^0 \to J/\psi\,p\pi^-$ decay.

This article reports the first observation of the $\Lambda_b^0 \to J/\psi\,p\pi^-$ decay and the determination of its branching fraction relative to the Cabibbo-favoured mode $\Lambda_b^0 \to J/\psi\,pK^-$. The latter, which was recently observed, has been used to obtain a precise measurement of the ratio of Λ_b^0 to B^0 lifetimes [3,9]. Its absolute branching ratio is yet to be determined. A measurement of the CP asymmetry difference between the $\Lambda_b^0 \to J/\psi\,p\pi^-$ and $\Lambda_b^0 \to J/\psi\,pK^-$ decays is also reported. The analysis is based on a data sample of proton-proton collisions, corresponding to an integrated luminosity of 1 fb^{-1} at a centre-of-mass energy of 7 TeV and 2 fb^{-1} at 8 TeV, collected with the LHCb detector.

2 Detector and software

The LHCb detector [16] is a single-arm forward spectrometer covering the pseudorapidity range $2 < \eta < 5$, designed for the study of particles containing b or c quarks. The detector includes a high-precision tracking system consisting of a silicon-strip vertex detector surrounding the proton-proton interaction region, a large-area silicon-strip detector located upstream of a dipole magnet with a bending power of about 4 Tm, and three stations of silicon-strip detectors and straw drift tubes [17] placed downstream of the magnet. The combined tracking system provides a momentum measurement with a relative uncertainty that varies from 0.4% at low momentum to 0.6% at 100 GeV/c, and an

impact parameter measurement with a resolution of 20 μm for charged particles with large transverse momentum, $p_{\rm T}$. Different types of charged hadrons are distinguished using information from two ring-imaging Cherenkov (RICH) detectors [18]. Photon, electron and hadron candidates are identified by a calorimeter system consisting of scintillating-pad and preshower detectors, an electromagnetic calorimeter and a hadronic calorimeter. Muons are identified by a system composed of alternating layers of iron and multiwire proportional chambers [19]. The trigger [20] consists of a hardware stage, based on information from the calorimeter and muon systems, followed by a software stage, which applies a full event reconstruction.

Candidate events are first required to pass the hardware trigger, which selects muons with $p_{\rm T} > 1.48\,{\rm GeV}/c$. In the subsequent software trigger, at least one of the candidate muons is required to be inconsistent with originating from any primary interaction. Finally, the muon pair is required to form a vertex that is significantly displaced from all primary vertices (PV) and to have a mass within 120 MeV/c^2 of the known J/ψ mass.

In the simulation, proton-proton collisions are generated using Pythia [21] with a specific LHCb configuration [22]. Decays of hadronic particles are described by EvtGen [23], in which final state radiation is generated using Photos [24]. The interaction of the generated particles with the detector and its response are implemented using the Geant4 toolkit [25] as described in Ref. [26].

3 Event Selection

The $\Lambda_b^0 \to J/\psi p\pi^-$ and $\Lambda_b^0 \to J/\psi pK^-$ decays are reconstructed with the J/ψ decaying to two muons. Charge conjugation is implied throughout except in the definition of the *CP* asymmetry.

Candidate $J/\psi \to \mu^+\mu^-$ decays are reconstructed from oppositely charged particles passing loose muon-identification requirements and with $p_{\rm T} > 500$ MeV/c. They are required to form a good quality vertex and have a mass in the range $[3030, 3150]$ MeV/c^2. This interval corresponds to about eight times the $\mu^+\mu^-$ mass resolution at the J/ψ mass and covers part of the J/ψ meson radiative tail.

Candidate Λ_b^0 baryons are selected from combinations of J/ψ candidates and two oppositely charged particles, one of which must be compatible with the proton hypothesis. The proton candidate is required to have a momentum, p, larger than 5 GeV/c, while the second charged particle must have $p > 3$ GeV/c. Both particles must have $p_{\rm T} > 500$ MeV/c and be inconsistent with coming from any PV. All four charged particles are required to be consistent with coming from a common vertex.

The reconstructed mass and decay time of the Λ_b^0 candidates are obtained from a kinematic fit [27] that constrains the mass of the $\mu^+\mu^-$ pairs to the known J/ψ mass and the Λ_b^0 candidate to originate from the PV. If the event has multiple PVs, all combinations are considered. Candidates are required to have a reconstructed decay time larger than 0.2 ps.

To remove backgrounds from $\Lambda_b^0 \to J/\psi\Lambda$ decays, candidates that have a $p\pi^-$ mass

within 5 MeV/c^2 of the Λ baryon mass are vetoed. To remove reflections from $B_s^0 \to J/\psi\,\phi$ decays, candidates are also vetoed if the hadron-pair mass is less than 1035 MeV/c^2 when applying a K^+ mass hypothesis to both particles.

The remaining candidates are split into samples of $\Lambda_b^0 \to J/\psi\, p\pi^-$ and $\Lambda_b^0 \to J/\psi\, pK^-$ according to the estimated probabilities that the charged meson candidate is a kaon or a pion. These probabilities are determined using a neural network (NN) exploiting information from the RICH detectors, calorimeter and muon systems, as well as track quality. Particles with a larger pion probability are treated as $\Lambda_b^0 \to J/\psi\, p\pi^-$ candidates, otherwise they are treated as $\Lambda_b^0 \to J/\psi\, pK^-$ candidates. In addition, the larger of these two probabilities is required to be in excess of 5%. The Λ_b^0 candidates are required to be in the mass range $[4900, 6100]$ MeV/c^2. After this selection 4.3×10^5 $\Lambda_b^0 \to J/\psi\, p\pi^-$ and 1.9×10^5 $\Lambda_b^0 \to J/\psi\, pK^-$ candidates remain.

The selection described above is not sufficient to isolate the small $\Lambda_b^0 \to J/\psi\, p\pi^-$ signal from the combinatorial background. The initial selection is therefore followed by a multivariate analysis, based on another NN [28]. The NN classifier's output is used as the final selection variable.

The NN is trained entirely on data, using the $\Lambda_b^0 \to J/\psi\, pK^-$ signal as a proxy for the $\Lambda_b^0 \to J/\psi\, p\pi^-$ decay. The training is performed using half of the $\Lambda_b^0 \to J/\psi\, pK^-$ candidates chosen at random. The other half is used to define the normalisation sample, allowing an unbiased measurement of the $\Lambda_b^0 \to J/\psi\, pK^-$ yield. The training uses signal and background weights determined using the *sPlot* technique [29] and obtained by performing a maximum likelihood fit to the unbinned mass distribution of the candidates meeting the loose selection criteria.

The fit probability density function (PDF) is defined as the sum of the Λ_b^0 signal component and the combinatorial background components. The parameterisation of the individual components is described in the next section.

Several reflections from B^0, B_s^0 and Λ_b^0 decays, reconstructed using misidentified particles, must be accounted for in the mass spectrum. In order to avoid the training being biased by these reflections, all candidates that have a mass compatible with the B^0, B_s^0 or Λ_b^0 mass after swapping the p and K assignments with any of π, K, or p are removed from the training.

The NN classifier uses information about the candidate kinematic distributions, vertex and track quality, impact parameter and particle identification information on the proton. The most discriminating quantities are the proton particle identification probability, the kinematic fit quality and the kaon separation of the PV in this order. The variables that are used in the NN are chosen to avoid correlations with the reconstructed Λ_b^0 mass and to have identical distributions in $\Lambda_b^0 \to J/\psi\, p\pi^-$ and $\Lambda_b^0 \to J/\psi\, pK^-$ simulated data.

Final selection requirements of the NN classifier output are chosen to optimise the expected statistical precision on the $\Lambda_b^0 \to J/\psi\, p\pi^-$ signal yield. The expected signal and background yields entering the sensitivity estimation are obtained from the training sample by scaling the number of surviving $\Lambda_b^0 \to J/\psi\, pK^-$ candidates by the expected yield based on an assumed branching fraction ratio of 0.1. The expected background is extrapolated from the number of $\Lambda_b^0 \to J/\psi\, p\pi^-$ candidates in the mass range $[5770, 6100]$ MeV/c^2. After

applying the final requirement on the NN classifier output, the multivariate selection rejects 99% of the background while keeping 75% of the $\Lambda_b^0 \to J/\psi p K^-$ signal, relative to the initial selection.

After applying the full selection, about 0.1% of the selected events have more than one candidate sharing at least one track, or more than one PV that can be used to determine the kinematic properties of the candidate. In these cases one of the candidates or PVs is used at random.

4 Signal and background description

For the candidates passing the NN requirements, the yields of $\Lambda_b^0 \to J/\psi p\pi^-$ and $\Lambda_b^0 \to J/\psi p K^-$ decays are determined from unbinned maximum likelihood fits to the mass distributions of reconstructed Λ_b^0 candidates. The PDF is defined as the sum of a Λ_b^0 signal component, a combinatorial background and the sum of several reflections.

The signal shape is parametrised by a Gaussian distribution with power-law tails on both sides, as indicated by simulation. The parameters describing the tails are taken from simulation, while the mean and width of the Gaussian are allowed to vary in the fit. The combinatorial background contribution is described by an exponential function, with yield and slope parameter allowed to vary freely.

Several peaking backgrounds due to decays of b hadrons to J/ψ mesons and two charged hadrons, where one or both hadrons are misidentified, survive the selection. In this fit they are not vetoed, unlike in the training of the NN, except for candidates consistent with the $B_s^0 \to J/\psi\phi$ hypothesis. Instead, their contribution is modelled by smoothed non-parametric functions determined from simulated data. The respective yields are determined by swapping the mass assignments of the p, π and K in turn and searching for peaks at the B^0, B_s^0 or Λ_b^0 masses. In the $\Lambda_b^0 \to J/\psi p\pi^-$ fit, significant backgrounds are found from the decays $\Lambda_b^0 \to J/\psi p K^-$ (with K^- identified as π^-), $B^0 \to J/\psi K^+\pi^-$ (with K^+ identified as p), and $B_s^0 \to J/\psi K^+K^-$ (with one K identified as p and the other as π). In the $\Lambda_b^0 \to J/\psi p K^-$ fit, the main contributions are from the decays $\overline{B}^0 \to J/\psi \pi^+ K^-$ (with π^+ identified as p), $B_s^0 \to J/\psi K^+K^-$ (with K^+ identified as p), and $\overline{\Lambda}_b^0 \to J/\psi \overline{p} K^+$ (with K^- and p swapped). These yields are then used as Gaussian constraints on the normalisation of the reflection background shapes. The results of the fits are shown in Fig. 1. The contributions of the reflections are summed, except for the large $\Lambda_b^0 \to J/\psi p K^-$ reflection in the $\Lambda_b^0 \to J/\psi p\pi^-$ fit, which is shown separately.

Low-mass contributions of partially reconstructed $\Lambda_b^0 \to J/\psi p\pi^-\pi^0$ and $\Lambda_b^0 \to J/\psi p K^-\pi^0$ decays, where the π^0 is not considered in the combination, are investigated. Adding such a component to the fit, with a mass shape taken from simulation, results in yields compatible with zero and does not change the signal yields.

In total $11\,179 \pm 109$ $\Lambda_b^0 \to J/\psi p K^-$ and 2102 ± 61 $\Lambda_b^0 \to J/\psi p\pi^-$ decays are obtained. The $\Lambda_b^0 \to J/\psi p K^-$ yield, having been determined on the half of the data not used in the training, is multiplied by two, resulting in a ratio of $\Lambda_b^0 \to J/\psi p\pi^-$ to $\Lambda_b^0 \to J/\psi p K^-$ yields of 0.0940 ± 0.0029.

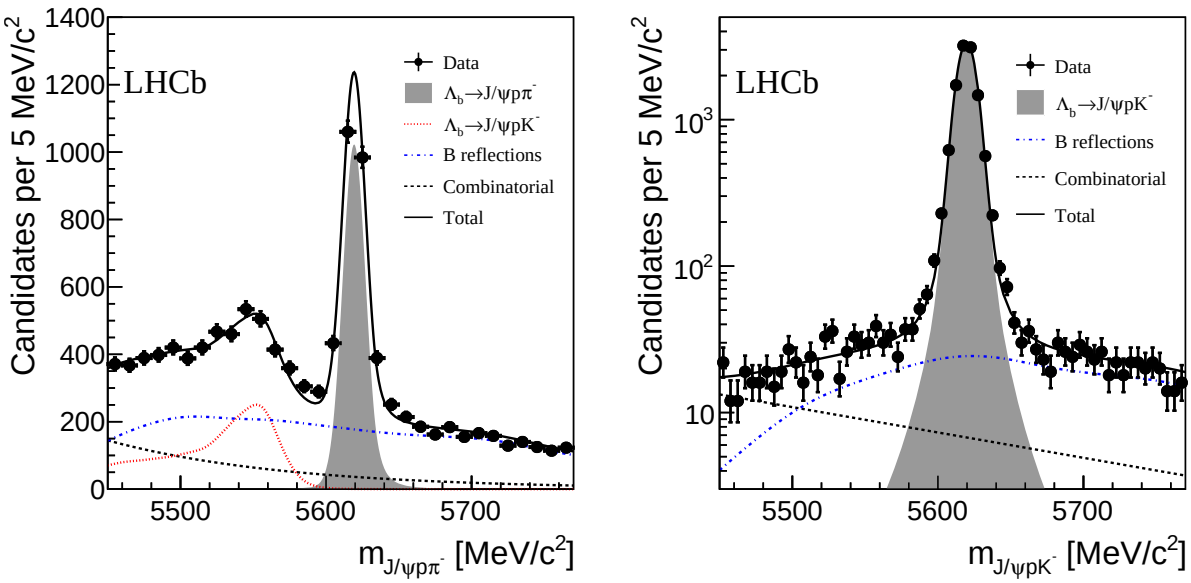

Figure 1: Distribution of (left) $J/\psi p\pi^-$ and (right) $J/\psi pK^-$ masses with fit projections overlaid. For $\Lambda_b^0 \to J/\psi pK^-$ candidates, only the normalisation sample is shown.

The shapes used in the mass fit are varied to determine a systematic uncertainty related to the mass model. No significant differences are found when trying alternate signal parameterisation that still result in a good fit. Changing the peaking backgrounds PDF, or letting their yield free in the fit, change their relative fit fractions, as well as that of the combinatorial background, but does not affect the signal yields. The combinatorial background model is changed from an exponential to a second-order polynomial, which results in a $\Lambda_b^0 \to J/\psi p\pi^-$ ($\Lambda_b^0 \to J/\psi pK^-$) yield reduced by 2.1% (0.3%). These variations are added in quadrature and used to estimate a systematic uncertainty on the ratio of branching fractions.

5 *CP* asymmetry

The same fit procedure is repeated separately for baryon (tagged by a positively charged proton) and antibaryon candidates. All parameters of the fits are determined again separately, except for the signal shape and the combinatorial background slope, which are taken from the fit to all candidates. A total of 1131 ± 40 $\Lambda_b^0 \to J/\psi p\pi^-$, 964 ± 38 $\overline{\Lambda}_b^0 \to J/\psi \overline{p}\pi^+$, 5655 ± 77 $\Lambda_b^0 \to J/\psi pK^-$ and 5529 ± 76 $\overline{\Lambda}_b^0 \to J/\psi \overline{p}K^+$ decays are found,

corresponding to the raw asymmetries

$$\begin{aligned}\mathcal{A}_{\rm raw}(\Lambda_b^0 \to J/\psi p\pi^-) &\equiv \frac{N(\Lambda_b^0 \to J/\psi p\pi^-) - N(\overline{\Lambda}_b^0 \to J/\psi \overline{p}\pi^+)}{N(\Lambda_b^0 \to J/\psi p\pi^-) + N(\overline{\Lambda}_b^0 \to J/\psi \overline{p}\pi^+)} \\ &= (+7.9 \pm 2.2)\%, \\ \mathcal{A}_{\rm raw}(\Lambda_b^0 \to J/\psi pK^-) &= (+1.1 \pm 0.9)\%.\end{aligned} \tag{1}$$

The procedure to assess the systematic uncertainties related to the shape of the mass distribution, described in Sec. 4, is repeated to determine the sensitivity of the raw asymmetries. A total variation of 0.7% is obtained, which is dominated by a change in $\mathcal{A}_{\rm raw}(\Lambda_b^0 \to J/\psi p\pi^-)$ when using a second-order polynomial background model.

The raw decay-rate asymmetry can be decomposed as

$$\mathcal{A}_{\rm raw}(\Lambda_b^0 \to J/\psi ph^-) = \mathcal{A}_{CP}(\Lambda_b^0 \to J/\psi ph^-) + \mathcal{A}_{\rm prod}(\Lambda_b^0) - \mathcal{A}_{\rm reco}(h^+) + \mathcal{A}_{\rm reco}(p), \tag{2}$$

where the terms on the right hand side of the equation are the *CP*-violating, Λ_b^0 production and reconstruction asymmetries of the hadron $h^\pm = \pi^\pm, K^\pm$ and the proton, respectively. Reconstruction asymmetries are defined following the convention $\mathcal{A}_{\rm reco}(h^+) \equiv \frac{\epsilon(h^+)-\epsilon(h^-)}{\epsilon(h^+)+\epsilon(h^-)}$ throughout, where ϵ is the reconstruction efficiency. The production asymmetry $\mathcal{A}_{\rm prod}$ and the proton reconstruction asymmetry cancel in the difference of the two asymmetries

$$\begin{aligned}\Delta\mathcal{A}_{CP} &\equiv \mathcal{A}_{CP}(\Lambda_b^0 \to J/\psi p\pi^-) - \mathcal{A}_{CP}(\Lambda_b^0 \to J/\psi pK^-) \\ &= \mathcal{A}_{\rm raw}(\Lambda_b^0 \to J/\psi p\pi^-) - \mathcal{A}_{\rm raw}(\Lambda_b^0 \to J/\psi pK^-) + \mathcal{A}_{\rm reco}(\pi^+) - \mathcal{A}_{\rm reco}(K^+).\end{aligned} \tag{3}$$

The kaon and pion asymmetries can be determined from the raw asymmetry of the $\overline{B}^0 \to J/\psi \overline{K}^*(892)^0$ decay with $\overline{K}^*(892)^0 \to K^-\pi^+$. It has been measured [30] as

$$\mathcal{A}_{\rm raw}(\overline{B}^0 \to J/\psi \overline{K}^*(892)^0) \equiv \frac{N(\overline{B}^0) - N(B^0)}{N(\overline{B}^0) + N(B^0)} = (-1.10 \pm 0.32 \pm 0.06)\%, \tag{4}$$

where the first uncertainty is statistical and the second systematic. It can be decomposed as

$$\begin{aligned}\mathcal{A}_{\rm raw}(\overline{B}^0 \to J/\psi \overline{K}^*(892)^0) &= \mathcal{A}_{CP}(\overline{B}^0 \to J/\psi \overline{K}^*(892)^0) - \kappa\mathcal{A}_{\rm prod}(B^0) \qquad (5) \\ &\quad + \mathcal{A}_{\rm reco}(\pi^+) - \mathcal{A}_{\rm reco}(K^+) \\ &\approx \mathcal{A}_{\rm reco}(\pi^+) - \mathcal{A}_{\rm reco}(K^+), \qquad (6)\end{aligned}$$

where κ is a dilution factor due to B^0 mixing and $\mathcal{A}_{\rm prod}(B^0)$ is the B^0 production asymmetry, which is compatible with zero [31]. Under the assumption of no *CP* asymmetry in the $\overline{B}^0 \to J/\psi \overline{K}^*(892)^0$ decay and negligible production asymmetry, this value can thus be taken as the combined kaon and pion reconstruction asymmetry, and is consistent with measurements in other decay modes to kaon and pions [31, 32].

The difference of *CP* asymmetries in the $\Lambda_b^0 \to J/\psi p\pi^-$ and $\Lambda_b^0 \to J/\psi pK^-$ decays can then be rewritten as

$$\begin{aligned}\Delta\mathcal{A}_{CP} &= \mathcal{A}_{\rm raw}(\Lambda_b^0 \to J/\psi p\pi^-) - \mathcal{A}_{\rm raw}(\Lambda_b^0 \to J/\psi pK^-) + \mathcal{A}_{\rm raw}(\overline{B}^0 \to J/\psi \overline{K}^*(892)^0) \quad (7)\\ &= (+5.7 \pm 2.4)\%,\end{aligned}$$

where the uncertainty is statistical only.

The kaon and pion momenta in Λ_b^0 decays are not identical to those in $\overline{B}^0 \to J/\psi \overline{K}^*(892)^0$ decays, which could induce different detector asymmetries in the Λ_b^0 and B^0 modes. This is investigated by weighting the $\Lambda_b^0 \to J/\psi p\pi^-$ and $\Lambda_b^0 \to J/\psi pK^-$ data to match the pion and kaon momentum distributions observed in $\overline{B}^0 \to J/\psi \overline{K}^*(892)^0$ decays. The value of $\Delta\mathcal{A}_{CP}$ changes by 0.8%, which is assigned as the systematic uncertainty related to reconstruction asymmetries.

Local *CP* asymmetries in the Dalitz plane are also searched for using the technique outlined in Ref. [33]. No significant local asymmetries are found.

6 Efficiency corrections and systematic uncertainties

The raw quantities need to be corrected to determine the physics quantities. The efficiency of the selection requirements is studied with simulation. Some quantities are known not to be well reproduced in simulation, namely the Λ_b^0 transverse momentum and lifetime, the particle multiplicity, and the $\Lambda_b^0 \to J/\psi p\pi^-$ and $\Lambda_b^0 \to J/\psi pK^-$ decay kinematic properties. For all these quantities the simulated data are weighted to match the observed distributions in data. They are obtained with the *sPlot* technique using the Λ_b^0 candidate mass as the control variable.

For three-body b-hadron decays, both the signal decays and the dominant combinatorial backgrounds populate regions close to the kinematic boundaries of the $J/\psi p\pi^-$ and $J/\psi pK^-$ Dalitz plot [34]. For more accurate modelling of these regions, it is convenient to transform the conventional Dalitz space to a rectangular space (hereafter referred to as the square Dalitz plot [35]). We follow the procedure described in Ref. [12].

The $\Lambda_b^0 \to J/\psi p\pi^-$ and $\Lambda_b^0 \to J/\psi pK^-$ decays have different detector acceptance, reconstruction and selection efficiencies. They are determined from simulated data, which are weighted to match the experimental data. The main differences are induced by

i. the detector acceptance, as the efficiency of $\Lambda_b^0 \to J/\psi pK^-$ is 6% larger than that for the $\Lambda_b^0 \to J/\psi p\pi^-$ decays due to the lower kinetic energy release in the former, which causes smaller opening angles;

ii. the reconstruction and preselection efficiency, which is 4% larger in $\Lambda_b^0 \to J/\psi p\pi^-$ decays due to the average total and transverse momentum of the final state particles being larger than in $\Lambda_b^0 \to J/\psi pK^-$ decays;

iii. the particle identification requirements on the π^- or K^-, which are more efficient on $\Lambda_b^0 \to J/\psi p\pi^-$ decays by 7%;

Table 1: Corrections and related systematic uncertainties on the ratio of $\Lambda_b^0 \to J/\psi p\pi^-$ to $\Lambda_b^0 \to J/\psi pK^-$ branching fractions (BF) and on the difference between the *CP* asymmetries $\Delta\mathcal{A}_{CP}$. The corrections are multiplicative on the branching fraction and additive for the asymmetry.

Source	BF	$\Delta\mathcal{A}_{CP}$
Simulation-based corrections	0.913 ± 0.040	-
PID	0.960 ± 0.010	-
Trigger	1.000 ± 0.010	-
Λ_b^0 lifetime	1.000 ± 0.001	-
Mass distribution model	1.000 ± 0.021	$0.0 \pm 0.7\%$
$\overline{B}^0 \to J/\psi\, \overline{K}^*(892)^0$	–	$-1.1 \pm 0.3\%$
Detection asymmetries	–	$0.0 \pm 0.8\%$
Total	0.876 ± 0.045	$-1.1 \pm 1.2\%$

iv. the ϕ veto, which removes 7% (3%) of the $\Lambda_b^0 \to J/\psi pK^-$ ($J/\psi p\pi^-$) signal.

Overall, these effects result in a further correction on the ratio of branching fractions of $\Lambda_b^0 \to J/\psi p\pi^-$ to $\Lambda_b^0 \to J/\psi pK^-$ decays of 0.913 ± 0.040.

The efficiency of particle identification is not perfectly modelled in simulation. The kaon and pion identification efficiencies are further weighted after the kinematic weighting described above, using a large sample of D^*-tagged $D^0 \to K^-\pi^+$ decays. The uncertainties are determined by varying the weights of the simulated data within their uncertainties, yielding a correction of 0.960 ± 0.010. The kinematic properties of the proton in the $\Lambda_b^0 \to J/\psi p\pi^-$ and $\Lambda_b^0 \to J/\psi pK^-$ decays are found to be the same. The same applies to the muons. The efficiencies of proton and muon identification therefore cancel in the ratio of branching fractions, as well as in the *CP* asymmetries.

The trigger efficiency is determined using simulation, which is validated using $\Lambda_b^0 \to J/\psi pK^-$ decays from data. Differences between the $\Lambda_b^0 \to J/\psi p\pi^-$ and $\Lambda_b^0 \to J/\psi pK^-$ decays efficiencies are at the percent level and are assigned as systematic uncertainties.

The value of the Λ_b^0 lifetime used in simulation is taken from Ref. [36], and is 3% lower than the current most precise measurement [3]. The simulated data is weighted to account for this and the difference is assigned as a systematic uncertainty.

The estimates of the systematic uncertainties described above are summarised in Table 1, along with the total obtained by summing them in quadrature. The uncertainty on the ratio of branching fractions is dominated by the uncertainty on corrections obtained from simulation, mostly due to the unknown decay kinematic properties of the $\Lambda_b^0 \to J/\psi p\pi^-$ decay. For $\Delta\mathcal{A}_{CP}$, the mass model distribution and the detection asymmetries contribute about equally.

7 Results and Conclusions

A signal of the Cabibbo-suppressed $\Lambda_b^0 \to J/\psi p\pi^-$ decay is observed for the first time using a data sample of proton-proton collisions at 7 and 8 TeV, corresponding to an integrated luminosity of 3 fb^{-1}. Applying the appropriate corrections detailed in Table 1, the ratio of branching fractions is measured to be

$$\frac{\mathcal{B}(\Lambda_b^0 \to J/\psi p\pi^-)}{\mathcal{B}(\Lambda_b^0 \to J/\psi pK^-)} = 0.0824 \pm 0.0025\,(\text{stat}) \pm 0.0042\,(\text{syst}).$$

Assuming these decays are dominated by tree $b \to c\bar{c}d$ and $b \to c\bar{c}s$ transitions, respectively, the ratio of Cabibbo-Kobayashi-Maskawa (CKM) matrix elements $|V_{cd}|^2/|V_{cs}|^2$ times ratio of phase space factors is approximately 0.08, compatible with the measured value. This ratio can also be compared to that of the decays $\Lambda_b^0 \to \Lambda_c^+ D^-$ and $\Lambda_b^0 \to \Lambda_c^+ D_s^+$, which involve the same quark lines as $\Lambda_b^0 \to J/\psi p\pi^-$ and $\Lambda_b^0 \to J/\psi pK^-$, respectively. The ratio of $\Lambda_b^0 \to \Lambda_c^+ D^-$ and $\Lambda_b^0 \to \Lambda_c^+ D_s^+$ has been measured as $0.042 \pm 0.003\,(\text{stat}) \pm 0.003\,(\text{syst})$ [11], which is consistent with this measurement, when taking into account the D^- and D_s^+ meson decay constants [36] and the different ratio of phase space factors.

Background-subtracted and efficiency-corrected distributions of kinematic distributions determined in the $\Lambda_b^0 \to J/\psi p\pi^-$ decay are shown in Fig. 2. In this case the Λ_b^0 mass is fixed to its known value and the kinematic properties recomputed [27]. No attempt is made to fit the decay rate on the Dalitz plane. The $p\pi^-$ mass distribution shows a rich resonant structure, as expected from fits to fixed-target experiment data [37, 38], and suggests the presence of the narrow $N(1520)$ or $N(1535)$, the $N(1650)$, as well as the broad $N(1440)$ resonances. No signs of exotic structures in the $J/\psi\,\pi^-$ or $J/\psi\,p$ mass distributions are seen. More data and further studies will be needed to inverstigate the underlying dynamics of this decay.

The *CP* asymmetry difference between the $\Lambda_b^0 \to J/\psi p\pi^-$ and $\Lambda_b^0 \to J/\psi pK^-$ decays is measured to be

$$\Delta A_{CP} = A_{CP}(\Lambda_b^0 \to J/\psi p\pi^-) - A_{CP}(\Lambda_b^0 \to J/\psi pK^-) = (+5.7 \pm 2.4\,(\text{stat}) \pm 1.2\,(\text{syst}))\%,$$

corresponding to a 2.2σ deviation from zero. No indications of large local *CP* asymmetries in the Dalitz plane are observed. The precision of these measurements illustrate the potential of Cabibbo-suppressed Λ_b^0 decays in studies of direct *CP* violation.

Acknowledgements

We express our gratitude to our colleagues in the CERN accelerator departments for the excellent performance of the LHC. We thank the technical and administrative staff at the LHCb institutes. We acknowledge support from CERN and from the national agencies: CAPES, CNPq, FAPERJ and FINEP (Brazil); NSFC (China); CNRS/IN2P3 (France); BMBF, DFG, HGF and MPG (Germany); SFI (Ireland); INFN (Italy); FOM and NWO (The Netherlands); MNiSW and NCN (Poland); MEN/IFA (Romania); MinES and FANO

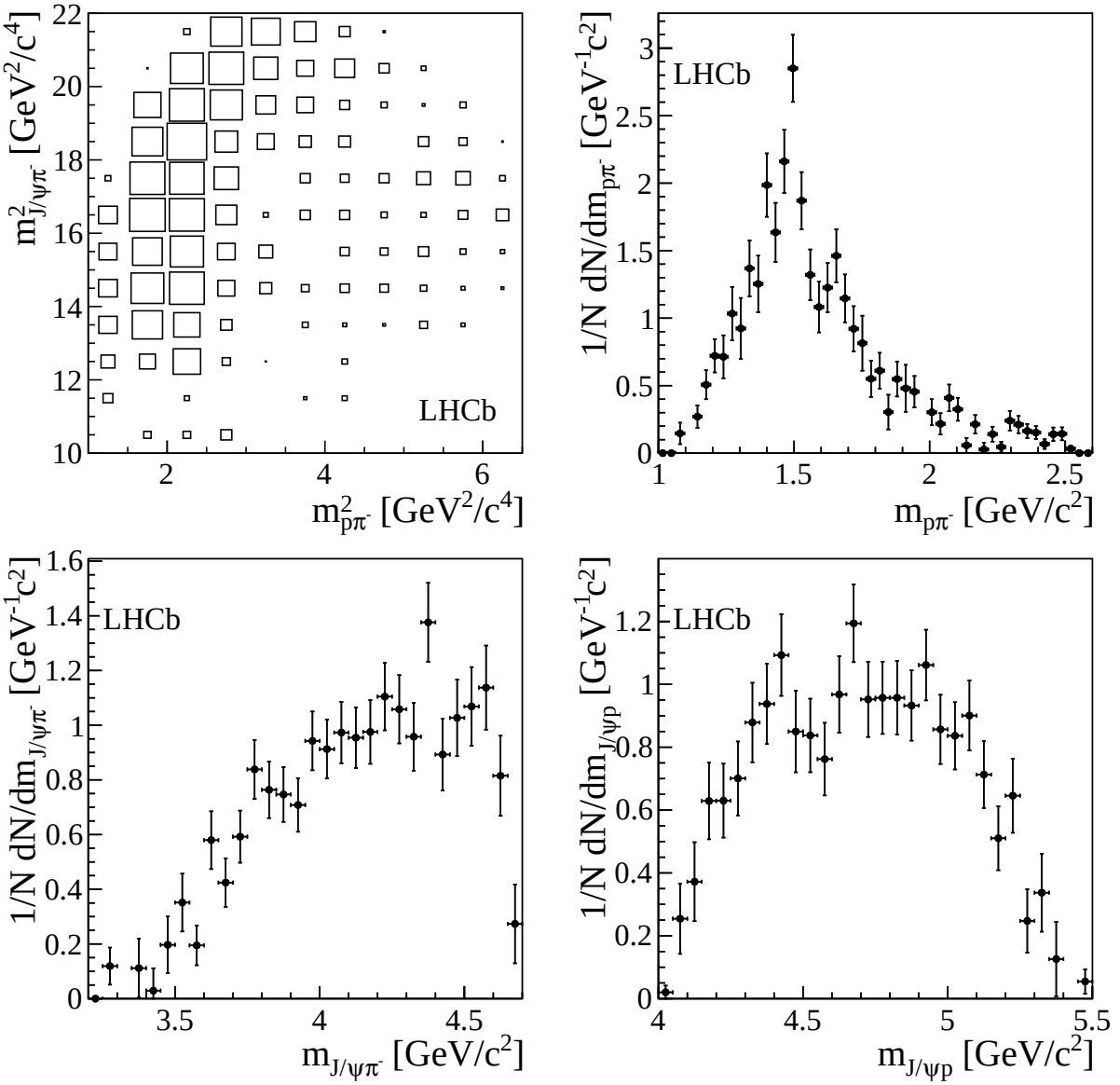

Figure 2: Efficiency-corrected and background-subtracted $\Lambda_b^0 \to J/\psi p\pi^-$ Dalitz plane and projections normalised to unit area on the $p\pi^-$, $J/\psi\,\pi^-$ and $J/\psi\,p$ axes.

(Russia); MinECo (Spain); SNSF and SER (Switzerland); NASU (Ukraine); STFC (United Kingdom); NSF (USA). The Tier1 computing centres are supported by IN2P3 (France), KIT and BMBF (Germany), INFN (Italy), NWO and SURF (The Netherlands), PIC (Spain), GridPP (United Kingdom). We are indebted to the communities behind the multiple open source software packages on which we depend. We are also thankful for the computing resources and the access to software R&D tools provided by Yandex LLC (Russia). Individual groups or members have received support from EPLANET, Marie

Skłodowska-Curie Actions and ERC (European Union), Conseil général de Haute-Savoie, Labex ENIGMASS and OCEVU, Région Auvergne (France), RFBR (Russia), XuntaGal and GENCAT (Spain), Royal Society and Royal Commission for the Exhibition of 1851 (United Kingdom).

References

[1] T. Mannel and S. Recksiegel, *Probing the helicity structure of $b \to s\gamma$ in $\Lambda_b^0 \to \Lambda\gamma$*, Acta Phys. Polon. **B28** (1997) 2489, arXiv:hep-ph/9710287; G. Hiller, M. Knecht, F. Legger, and T. Schietinger, *Photon polarization from helicity suppression in radiative decays of polarized Λ_b to spin-3/2 baryons*, Phys. Lett. **B649** (2007) 152, arXiv:hep-ph/0702191.

[2] LHCb collaboration, R. Aaij *et al.*, *Study of the kinematic dependences of Λ_b^0 production in pp collisions and a measurement of the $\Lambda_b^0 \to \Lambda_c^+\pi^-$ branching fraction*, arXiv:1405.6842, submitted to JHEP; LHCb collaboration, R. Aaij *et al.*, *Measurement of b hadron production fractions in 7 TeV pp collisions*, Phys. Rev. **D85** (2012) 032008, arXiv:1111.2357.

[3] LHCb collaboration, R. Aaij *et al.*, *Precision measurement of the ratio of the Λ_b^0 to $\bar{B}^0$ lifetimes*, Phys. Lett. **B734** 122, arXiv:1402.6242.

[4] LHCb collaboration, R. Aaij *et al.*, *Measurements of the B^+, B^0, B_s^0 meson and Λ_b^0 baryon lifetimes*, JHEP **04** (2014) 114, arXiv:1402.2554; CMS collaboration, S. Chatrchyan *et al.*, *Measurement of the Λ_b^0 lifetime in pp collisions at $\sqrt{s} = 7$ TeV*, JHEP **07** (2013) 163, arXiv:1304.7495.

[5] ATLAS collaboration, G. Aad *et al.*, *Measurement of the Λ_b lifetime and mass in the ATLAS experiment*, Phys. Rev. **D87** (2013) 032002, arXiv:1207.2284.

[6] LHCb collaboration, R. Aaij *et al.*, *Measurements of the Λ_b^0, Ξ_b^- and Ω_b^- baryon masses*, Phys. Rev. Lett. **110** (2013) 182001, arXiv:1302.1072.

[7] LHCb collaboration, R. Aaij *et al.*, *Observation of excited Λ_b^0 baryons*, Phys. Rev. Lett. **109** (2012) 172003, arXiv:1205.3452.

[8] LHCb collaboration, R. Aaij *et al.*, *Measurements of the $\Lambda_b^0 \to J/\psi\Lambda$ decay amplitudes and the Λ_b^0 polarisation in pp collisions at $\sqrt{s} = 7$ TeV*, Phys. Lett. **B724** (2013) 27, arXiv:1302.5578.

[9] LHCb collaboration, R. Aaij *et al.*, *Precision measurement of the Λ_b^0 baryon lifetime*, Phys. Rev. Lett. **111** (2013) 102003, arXiv:1307.2476.

[10] LHCb collaboration, R. Aaij *et al.*, *Study of beauty baryon decays to D^0ph^- and $\Lambda_c^+h^-$ final states*, Phys. Rev. **D89** (2014) 032001, arXiv:1311.4823.

[11] LHCb collaboration, R. Aaij *et al.*, *Study of beauty hadron decays into pairs of charm hadrons*, Phys. Rev. Lett. **112** (2014) 202001, arXiv:1403.3606.

[12] LHCb collaboration, R. Aaij *et al.*, *Searches for Λ_b^0 and Ξ_b^0 decays to $K^0_S p\pi^-$ and $K^0_S pK^-$ final states with first observation of the $\Lambda_b^0 \to K^0_S p\pi^-$ decay*, JHEP **04** (2014) 087, arXiv:1402.0770.

[13] LHCb collaboration, R. Aaij *et al.*, *Measurement of the differential branching fraction of the decay $\Lambda_b^0 \to \Lambda\mu^+\mu^-$*, Phys. Lett. **B725** (2013) 25, arXiv:1306.2577.

[14] CDF collaboration, T. A. Aaltonen *et al.*, *Measurements of Direct CP-Violating Asymmetries in Charmless Decays of Bottom Baryons*, arXiv:1403.5586.

[15] K. De Bruyn, R. Fleischer, and P. Koppenburg, *Extracting γ and penguin topologies through CP violation in $B_s^0 \to J/\psi K^0_{\rm S}$*, Eur. Phys. J. **C70** (2010) 1025, arXiv:1010.0089; S. Faller, R. Fleischer, and T. Mannel, *Precision physics with $B_s^0 \to J/\psi\phi$ at the LHC: the quest for New Physics*, Phys. Rev. **D79** (2009) 014005, arXiv:0810.4248.

[16] LHCb collaboration, A. A. Alves Jr. *et al.*, *The LHCb detector at the LHC*, JINST **3** (2008) S08005.

[17] R. Arink *et al.*, *Performance of the LHCb Outer Tracker*, JINST **9** (2014) P01002, arXiv:1311.3893.

[18] M. Adinolfi *et al.*, *Performance of the LHCb RICH detector at the LHC*, Eur. Phys. J. **C73** (2013) 2431, arXiv:1211.6759.

[19] A. A. Alves Jr. *et al.*, *Performance of the LHCb muon system*, JINST **8** (2013) P02022, arXiv:1211.1346.

[20] R. Aaij *et al.*, *The LHCb trigger and its performance in 2011*, JINST **8** (2013) P04022, arXiv:1211.3055.

[21] T. Sjöstrand, S. Mrenna, and P. Skands, *PYTHIA 6.4 physics and manual*, JHEP **05** (2006) 026, arXiv:hep-ph/0603175; T. Sjöstrand, S. Mrenna, and P. Skands, *A brief introduction to PYTHIA 8.1*, Comput. Phys. Commun. **178** (2008) 852, arXiv:0710.3820.

[22] I. Belyaev *et al.*, *Handling of the generation of primary events in* Gauss*, the LHCb simulation framework*, Nuclear Science Symposium Conference Record (NSS/MIC) **IEEE** (2010) 1155.

[23] D. J. Lange, *The EvtGen particle decay simulation package*, Nucl. Instrum. Meth. **A462** (2001) 152.

[24] P. Golonka and Z. Was, *PHOTOS Monte Carlo: a precision tool for QED corrections in Z and W decays*, Eur. Phys. J. **C45** (2006) 97, arXiv:hep-ph/0506026.

[25] Geant4 collaboration, J. Allison *et al.*, *Geant4 developments and applications*, IEEE Trans. Nucl. Sci. **53** (2006) 270; Geant4 collaboration, S. Agostinelli *et al.*, *Geant4: a simulation toolkit*, Nucl. Instrum. Meth. **A506** (2003) 250.

[26] M. Clemencic *et al.*, *The LHCb simulation application,* GAUSS*: design, evolution and experience*, J. Phys. Conf. Ser. **331** (2011) 032023.

[27] W. D. Hulsbergen, *Decay chain fitting with a Kalman filter*, Nucl. Instrum. Meth. **A552** (2005) 566, arXiv:physics/0503191.

[28] M. Feindt, *A neural Bayesian estimator for conditional probability densities*, arXiv:physics/0402093.

[29] M. Pivk and F. R. Le Diberder, *sPlot: a statistical tool to unfold data distributions*, Nucl. Instrum. Meth. **A555** (2005) 356, arXiv:physics/0402083.

[30] LHCb collaboration, R. Aaij *et al.*, *Measurement of the CP asymmetry in $B^0 \to K^{*0}\mu^+\mu^-$ decays*, Phys. Rev. Lett. **110** (2013) 031801, arXiv:1210.4492.

[31] LHCb collaboration, R. Aaij *et al.*, *First observation of CP violation in the decays of B_s^0 mesons*, Phys. Rev. Lett. **110** (2013) 221601, arXiv:1304.6173.

[32] LHCb collaboration, R. Aaij *et al.*, *Measurement of CP asymmetry in $D^0 \to K^-K^+$ and $D^0 \to \pi^-\pi^+$ decays*, arXiv:1405.2797, submited to PLB.

[33] I. Bediaga *et al.*, *Second generation of 'Miranda procedure' for CP violation in Dalitz studies of B, (D & τ) decays*, Phys. Rev. **D86** (2012) 036005, arXiv:1205.3036; I. Bediaga *et al.*, *On a CP anisotropy measurement in the Dalitz plot*, Phys. Rev. **D80** (2009) 096006, arXiv:0905.4233.

[34] R. Dalitz, *On the analysis of tau-meson data and the nature of the tau-meson*, Phil. Mag. **44** (1953) 1068.

[35] BaBar collaboration, B. Aubert *et al.*, *An amplitude analysis of the decay $B^\pm \to \pi^\pm\pi^\pm\pi^\mp$*, Phys. Rev. **D72** (2005) 052002, arXiv:hep-ex/0507025.

[36] Particle Data Group, J. Beringer *et al.*, *Review of particle physics*, Phys. Rev. **D86** (2012) 010001, and 2013 partial update for the 2014 edition.

[37] A. Anisovich *et al.*, *Properties of baryon resonances from a multichannel partial wave analysis*, Eur. Phys. J. **A48** (2012) 15, arXiv:1112.4937.

[38] R. Arndt, W. Briscoe, I. Strakovsky, and R. Workman, *Extended partial-wave analysis of πN scattering data*, Phys. Rev. **C74** (2006) 045205, arXiv:nucl-th/0605082.